Applied Vegetation Science **19** (2016) 132–146

Evaluating an unmanned aerial vehicle-based approach for assessing habitat extent and condition in fine-scale early successional mountain mosaics

João Gonçalves, Renato Henriques, Paulo Alves, Rita Sousa-Silva, António T. Monteiro, Ângela Lomba, Bruno Marcos & João Honrado

Keywords
Habitat types; Image classification; Monitoring; Mountain system; Natura 2000; Random forest; Remote sensing; Unmanned aerial vehicle; Very high spatial resolution

Nomenclature
Castroviejo (1986–2013) for published volumes, Franco (1984) and Franco & Afonso (1998) for other groups, except *Agrostis* (Romero García et al. 1988)

Abbreviations
DSM = digital surface model; EU = European Union; GCP = ground control points; GPS = differential global positioning system; UAV = unmanned aerial vehicle; RF = random forest

Received 6 October 2014
Accepted 18 September 2015
Co-ordinating Editor: Duccio Rocchini

Gonçalves, J. (corresponding author, jfgoncalves@fc.up.pt)[1,2],
Henriques, R. (rhenriques@dct.uminho.pt)[3],
Alves, P. (paulo.alves@fc.up.pt)[1],
Sousa-Silva, R. (anarita.silva@ees.kuleuven.be)[4],
Monteiro, A.T. (amonteiro@fc.up.pt)[1],
Lomba, Â. (angelalomba@fc.up.pt)[1],
Marcos, B. (bruno.marcos@cibio.up.pt)[1],
Honrado, J. (jhonrado@fc.up.pt)[1,2]

[1]InBIO, Research Network in Biodiversity and Evolutionary Biology Associate Laboratory, CIBIO, Research Center in Biodiversity and Genetic Resources, Predictive Ecology Group, Campus Agrário de Vairão, R. Padre Armando Quintas, N° 7, 4485-661 Vairão, Portugal;
[2]Faculty of Sciences, University of Porto, Rua Campo Alegre s/n, 4169-007 Porto, Portugal;
[3]Institute of Earth Sciences (ICT/University of Minho/CCT), Campus de Gualtar, 4710-057 Braga, Portugal;
[4]Division Forest Nature and Landscape, Department of Earth and Environmental

Abstract

Question: Can very high-resolution colour orthophotography and digital surface models (DSMs) from an unmanned aerial vehicle (UAV) be effectively used for assessment of habitat extent and condition in fine-scale disturbance-dependent mosaics?

Location: *Serra de Arga* mountain range, a Natura 2000 protected site in the NW region of Portugal where drastic changes in pastoral activities have occurred over recent decades.

Methods: An UAV platform was used to collect very high-resolution (6 cm) images and to produce a DSM (10 cm). From these data, several features were extracted related to colour, band ratios, as well as texture features calculated from colour imagery and surface elevation. Based on a systematic sampling design, field data were collected for both training and validation of a supervised classifier. Extracted features and ground truth training data were combined to calibrate a pixel-based Random forest classifier, with the purpose of devising a habitat map for the entire study area. Map validation was performed to assess classification accuracy, and feature importance metrics were calculated.

Results: Validation results revealed good mean overall accuracy (0.89), with some performance decrease in situations of high interspersion of habitat types. The priority habitat type 6230* (*Nardus* grasslands), defining the vegetation matrix of the test site, obtained 0.96 and 0.91, considering, respectively, producer and user accuracy. In turn, priority habitat type 4020* (Atlantic wet heathlands) recorded 0.68 and 0.77. The obtained habitat map allowed measurement of the extent, description of the spatial arrangement and provided an indication of the conservation condition of target habitat types. Test results regarding the discrimination ability of different features highlighted the importance of surface elevation textures derived from the DSM, followed by band ratios textures and other more complex texture features calculated from colour imagery.

Conclusions: Overall, the developed methodology showed promising results for assessing the extent and condition of habitats of high conservation priority in fine-scale, dynamic vegetation mosaics. Future advances in the use of UAV platforms may play an important role in monitoring protected sites and fulfil legal reporting obligations of EU member states, while reducing the costs associated with intensive in-field assessments.

Applied Vegetation Science
Doi: 10.1111/avsc.12204

Sciences, Katholieke Universiteit Leuven,
Celestijnenlaan 200E, 3001, Leuven, Belgium

Introduction

The continuous monitoring of species and habitats of high conservation value across Natura 2000 protected areas is an obligation established under the Habitats Directive across the European Union (European Commission 1992). It is also a requirement in order to tackle human-driven land-use changes, which severely impact terrestrial biodiversity and are expected to affect it considerably throughout the next 100 yrs (Sala et al. 2000; Waldhardt et al. 2004). A large part of these protected areas is located in mountainous regions, including marginal Mediterranean mountains currently affected by socio-economic changes (Bolliger et al. 2007). These cultural landscapes, frequently exhibiting high levels of biological diversity (Bielsa et al. 2005; Brown et al. 2011), currently face shifts in agricultural practices and human inputs, varying from partial abandonment of some parcels, creating a landscape mosaic of unused and cropped areas (Bielsa et al. 2005), to total abandonment of agriculture (and pastoralism) and progressive transformation into uncultivated land (MacDonald et al. 2000). This usually leads to an increase in the area occupied by semi-natural vegetation, such as scrubland and woodland (Bielsa et al. 2005), and a gradual colonization by non-crop species, initially with annual herbaceous plants (mainly ruderal species), which are gradually replaced by perennial herbs and low shrubs, creating conditions for the development of taller woody species that ultimately cause the loss of open habitats (Plieninger 2006).

In such context, the Natura 2000 network represents a key instrument to preserve the high nature value occurring on small-scale and actively managed habitats under threat due to abandonment of farming and grazing activity. However, monitoring the extent and condition of disturbance-dependent habitat types is particularly challenging as they often occur in fine-grained, highly dynamic mosaics maintained through extensive farming and/or moderate grazing pressure (Halada et al. 2011). Monitoring strategies are even more challenging under a scenario of widespread abandonment of husbandry in marginal rural areas, since these habitats will have their occupancy area reduced due to successional evolution towards scrub or woodland, especially in regions where the wild herbivore fauna has been depleted by centuries of human land management (Goodall & Perry 2009). In addition, changes in fire regimes triggered by shrub encroachment and fuel biomass accumulation are another threat to these habitats (Burkinshaw & Bork 2009).

Currently, national and regional authorities liable to provide assessment of the distribution and extent of Annex I habitats are faced with urgent data needs yet limited means to acquire data (Weiers et al. 2004; Vanden Borre et al. 2011; Spanhove et al. 2012). As financial resources are limited, the monitoring approaches need to be as cost-effective and consistent as possible. As such, remote sensing techniques have emerged as a powerful tool for habitat mapping and monitoring (Weiers et al. 2004; Vanden Borre et al. 2011; Nagendra et al. 2013; Corbane et al. 2015). The analysis of high spatial resolution aerial photography is commonly used for vegetation classification and species identification (González-Orozco et al. 2010), however the resolution of these image sensors is usually insufficient to provide accurate quantifications of small-scale and complex habitats, thus it is essential to use more advanced systems (Gross et al. 2009; Vanden Borre et al. 2011). Recent advances in the use of very high-spatial resolution satellite imagery (e.g. RapidEye, QuickBird) have proven highly useful for mapping Natura 2000 habitat types, such as grasslands (Hernando et al. 2012; Schmidt et al. 2014; Buck et al. 2015) and heathlands (Förster et al. 2008). In addition, developments in unmanned aerial vehicles (UAVs) for environmental remote sensing purposes have provided the means for achieving accuracies that meet or exceed traditional aerial photo-interpretation techniques (Knoth et al. 2013; Husson et al. 2014). The low flight altitude relative to other aircraft and satellites, the reduced or absence of cloud contamination, as well as their fine resolution and flexible scheduling of flight missions allows UAVs to provide visual imagery at a more localized and biologically distinguishable level, thus bridging the gap between ground-based observations and lower resolution remotely sensed data (Laliberte & Rango 2008; Getzin et al. 2012). Moreover, UAV platforms allow information to be obtained in problematic areas of accessibility, such as bogs, cliffs (Knoth et al. 2013), riverine or lake ecosystems (Husson et al. 2014).

Despite all the above advantages, major challenges still exist in data processing, namely image classification procedures (Huang et al. 2007) due to the large amount of data stored during flight missions (Permuter et al. 2006). Automated or semi-automated classification methods are therefore crucial for UAV applications in ecology and other

Doi: 10.1111/avsc.12204

fields. In this respect, a plethora of classification methods have been developed with Random Forest (hereafter RF; Breiman (2001)), a powerful machine learning technique, becoming increasingly popular in remote sensing applications (Pal 2005; Immitzer et al. 2012; Rodriguez-Galiano et al. 2012). Several studies have shown that RF performs better than other classification algorithms (Rodriguez-Galiano & Chica-Rivas 2012; Rodriguez-Galiano et al. 2012; Zhang & Xie 2013), with strong ability to handle high-dimensional data sets, making it attractive for processing high spatial resolution data.

In this study, focused on disturbance-dependent habitat mosaics in a Natura 2000 site, we tested an UAV-based methodology for assessing complex, dynamic vegetation mosaics composed of several EU habitat types of high conservation value, including two considered of high priority (Atlantic wet heath and *Nardus* grasslands). We discuss the classification performance and suitability of this approach to support the assessment and monitoring of habitat types with high conservation value, with a reduction in running costs and operational complexity of image acquisition with UAV technologies.

Methods

Study area and focal habitat mosaic

The study area is located in the Serra de Arga mountain range (Fig. 1), a Natura 2000 site located in the northwest region of Portugal (8°42′39.662″ W, 41°49′13.890″ N), comprising a total area of 9.72 ha. Elevation ranges from 747 to 781 m a.s.l. and the climate is cool summer Mediterranean type Csb according to the Köppen-Geiger classification system (Peel et al. 2007). Total annual precipitation is 1510 mm and minimum, average and maximum annual temperatures are, respectively: 6.1, 11.7 and 17.4 °C (Ninyerola et al. 2005).

This area is characterized by a mosaic, dominated by two different types of vegetation, corresponding to two priority habitat types listed in Annex I of the EU Habitats Directive (see Fig. 2 and Appendix S1): Atlantic wet heathlands (habitat 4020*) and *Nardus* grasslands (habitat 6230*). Habitat type 4020* (Temperate Atlantic wet heaths with *Erica ciliaris* and *Erica tetralix*) corresponds to dense formations on wet acid soils, dominated by different species of heather (*E. ciliaris*, *E. tetralix*, *Calluna vul-*

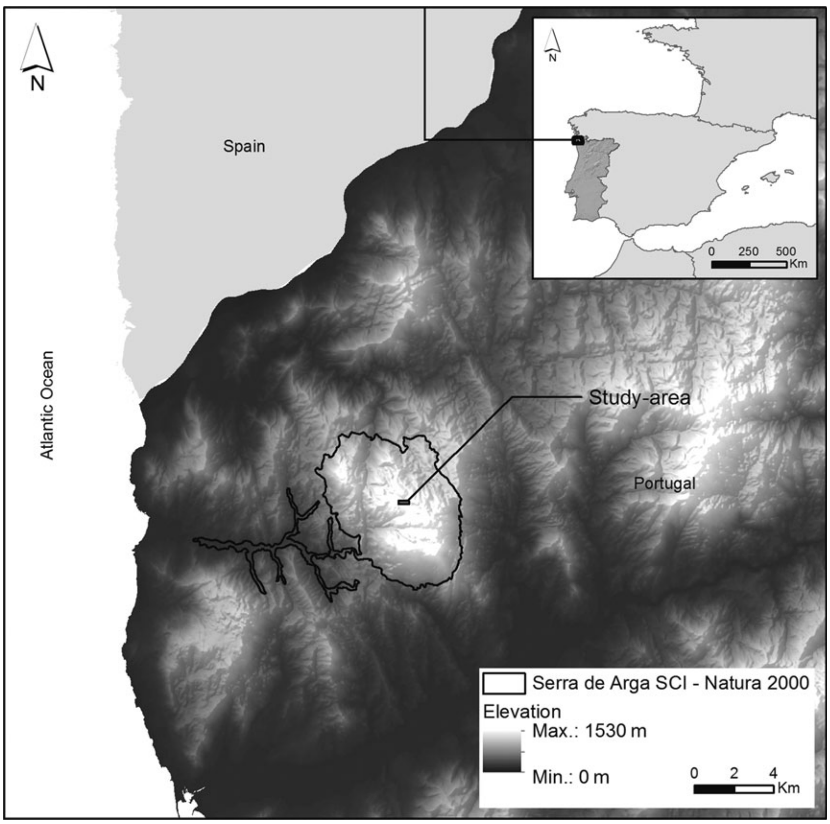

Fig. 1. Study area location in the Iberian Peninsula and the NW region of Portugal. The test site is fully included in the Natura 2000 *Serra de Arga* Site of Community Importance.

Applied Vegetation Science
Doi: 10.1111/avsc.12204

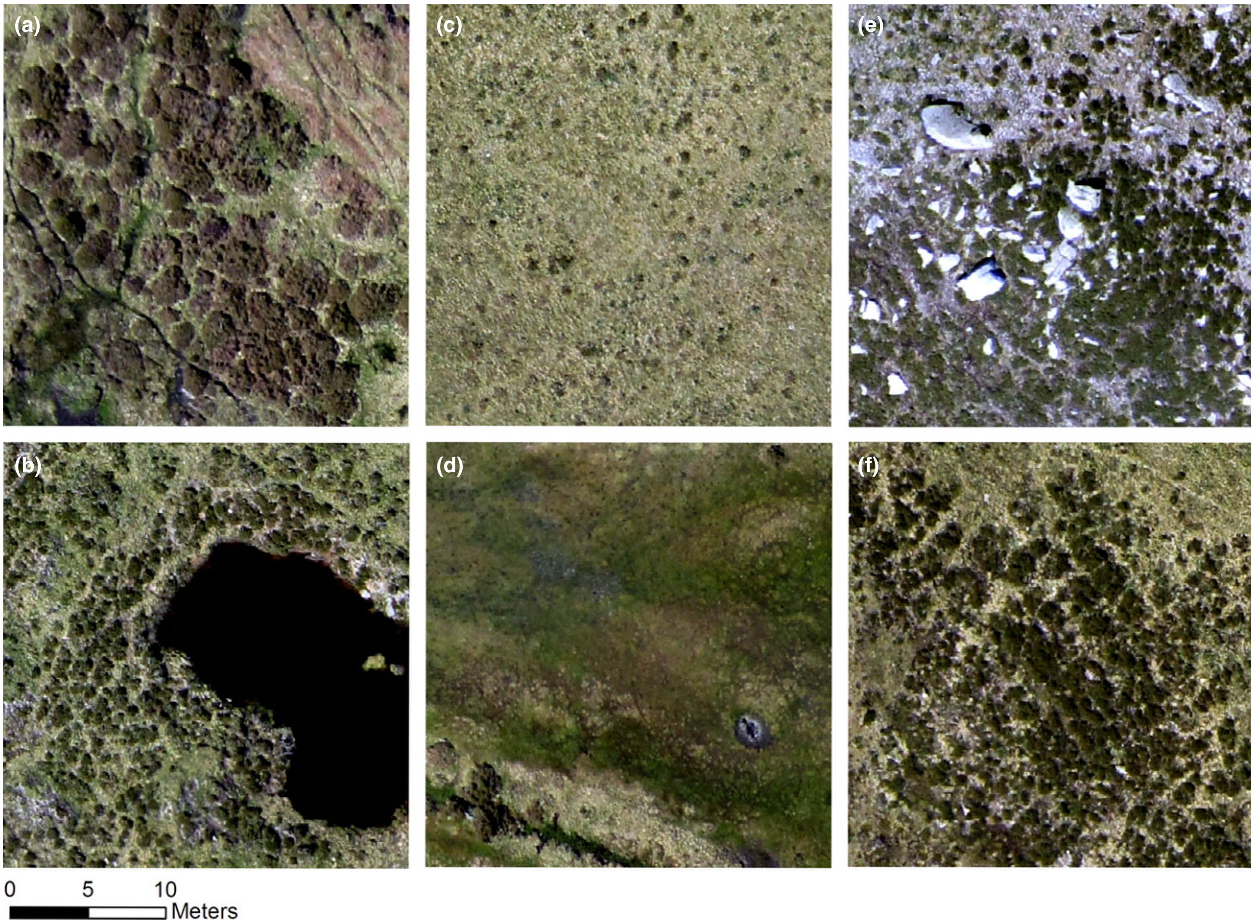

Fig. 2. The focal habitats as captured by the UAV platform. (**a**) Wet heath, habitat type 4020*, in dense/large shrub formations in concave/wet areas; (**b**) habitat 4020* around a small pond; (**c**) continuous, species-rich *Nardus* grasslands, habitat type 6230*, with low shrub density; (**d**) 6230* habitat with bare soil, highlighting poor habitat condition; (**e**) dry heath, habitat type 4030, in a mosaic with bare rock/soil areas; (**f**) heath (4030) encroachment on *Nardus* grassland denoting degradation due to decreased grazing pressure.

garis) and gorse (*Ulex minor*) and hygrophilous species of *Genista* (*G. anglica*, *G. micrantha*). This habitat type may include various densities of grass and occasional bare soil, depending on local conditions and disturbances. Habitat type 6230* (Species-rich *Nardus* grassland, on siliceous substrates in mountain areas and sub-mountain areas in continental Europe) is dominated by perennial grasses and rushes (*Nardus stricta*, *Danthonia decumbens*, *Juncus squarrosus*, *Agrostis hesperica*), usually accompanied by several small-sized forbs (*Serratula tinctoria* subsp. *seoanei*, *Polygala serpyllifolia*, *Galium saxatile*). Heath shrubs may occur as scattered plants or small patches, but the grassland component is typically dominant except in degraded forms of the habitat. In this case, shrubs and bare soil will become more abundant and the typical vegetation structure and species assembly will be depleted. In this southern limit of their distribution, these two habitat types occur in dense, dynamic mosaics on wet oligotrophic soils, usually on high plains and near springs. Small ponds or streams, dry heath (habitat 4030) and areas of bare ground (soil or rock) are other, less frequent components of the mosaic.

The composition and conservation value of the mosaic depends on the disturbance regime, especially on grazing pressure. Thus, low levels of grazing will favour wet heath, which becomes the vegetation habitat type. Conversely, high levels of grazing will favour *Nardus* grasslands, however intensive grazing will reduce their species diversity and conservation value, and may even trigger its replacement by other vegetation types more adapted to heavy loads of grazing, such as species-poor grasslands dominated by *Agrostis capillaris*. On the other hand, no grazing or even very low pressure will allow scrub encroachment and a decrease in the extent of both habitat types. The fact that this and other mountainous areas in the region have undergone changes in pastoral activities (namely aban-

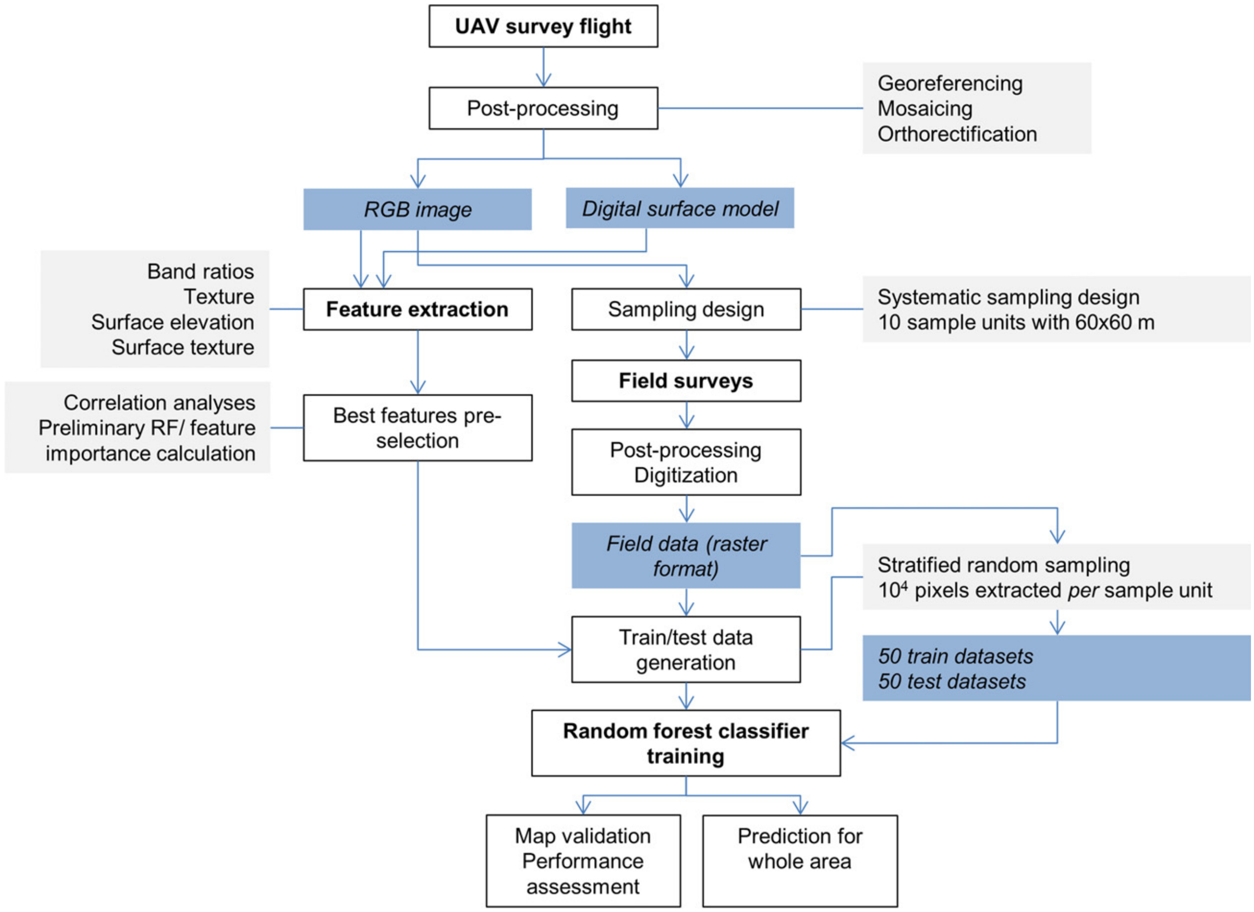

Fig. 3. Overview of the methodological approach tested. The scheme uses dashed boxes to denote processes (bold letters signal important processing steps), grey boxes denote specific or detailed aspects for certain processes and blue boxes indicate data.

donment of husbandry and local concentration of grazing pressure) over recent decades justifies our use of this site for testing the methodology.

Aerial imagery and surface elevation data acquisition and pre-processing

The general workflow of the tested methodology is illustrated in Fig. 3 and included several steps for imagery acquisition, post-processing, feature extraction and selection, sampling design and field survey and, finally, image classification and validation.

The workflow started with the acquisition of very high-resolution aerial images (6 cm·pixel^{-1}) at the beginning of spring 2013 (17 Apr) using a SenseFly-SwingletCAM UAV platform equipped with a Canon Ixus 220 HS digital camera with 12 MP sensor (4000 × 3000 pixels). Although spectral sensitivity data for this camera were unavailable from the UAV manufacturer, we compared it to 12 Canon models and calculated the average band centres (±SE) for the red, green and blue bands (see Appendix S2 for more details). These were located, respectively, at: 594 ± 2, 527 ± 2 and 462 ± 2 nm; overall the green band exhibited higher relative spectral sensitivity, a common feature in commercial digital sensors (Campbell & Wynne 2011). The flight was performed at 15:00 h under clear sky conditions at an altitude of approximately 940 m. Additional flight parameters, such as image overlap (set to 60% and 70% in the X and Y directions, respectively), study area limits and spatial resolution were set and uploaded to the device's internal memory.

Before the flight, the terrain was prepared with visible targets, later used as ground control points (GCP) for georeferencing the aerial photographs and the digital surface model (DSM). GCP positioning was collected with a Trimble 5800 RTK dual frequency DGPS with a positional error below 20 mm.

The photogrammetric processing, orthorectification and mosaicing were performed with PhotoScan software (Agisoft 2012), allowing us to obtain a very high resolution

Applied Vegetation Science
Doi: 10.1111/avsc.12204

DSM with 10 cm·pixel^{-1} and an orthorectified image with a RMSE equal to 0.628 pixel^{-1} in GeoTIFF format, using the WGS1984 geographic coordinate system.

Sampling design and in-field data collection for training and validation

Training data are required for calibrating supervised classification algorithms such as RF. In order to obtain these data we employed a design-based systematic sampling strategy (Gruijter et al. 2006) with ten regularly spaced sample units with 60 × 60 m covering approximately 37% of the study area (Fig. 4). Systematic sampling allows uniform coverage with generally more efficient and accurate results than simple random sampling, and also presents operational advantages, since regularity of the grid decreased the time required to locate and move between consecutive plots during fieldwork (Gruijter et al. 2006; Köhl et al. 2006). Field surveys were used to collect ground truth training/validation data, and started after defining a suitable map legend including all observable classes in the previously obtained UAV colour image. The implemented protocol was based on a fine-scale in-field photo-interpretation (over the UAV colour images) of each sample unit by delineating each homogeneous patch pertaining to a given dominant class. The minimum mapping unit was set to 0.36 m^2 due to the very high spatial resolution of the obtained orthophotos (6 cm·pixel^{-1}) and the fine-scale patchiness of vegetation. This field mapping procedure was supported by previously defined spatial and thematic criteria, thus standardizing collection processes. Field collected data was later digitized and corrected in a GIS environment.

Feature extraction

In order to test the usefulness of colour imagery and the DSM obtained from the UAV platform, we calculated several colour, band ratios and textures, as well as, surface elevation, curvature and surface texture features from these data. A total of 176 features were obtained (see examples in Fig. 5; the complete list of features is presented in Appendix S3). Colour features were obtained directly from digital number values for the red (R), green (G) and blue (B) channels. Texture features using individual R, G and B channels were extracted by calculating the mean, variance, skewness and kurtosis for three different kernel sizes: 3 × 3, 5 × 5 and 9 × 9 pixels. Kernel sizes were selected based on a preliminary visual inspection of image patterns, balancing the ability to identify different vegetation/habitat types (and their edges) with the loss of detail when increasing kernel size.

Additionally, band ratios were calculated by performing simple algebraic operations based on combinations of colour channels, e.g.: R/G, R/B, R/(G+B), R/(R+G+B). Using each calculated band ratio, texture features were also extracted by calculating the mean and variance for two different kernel sizes: 5 × 5 and 11 × 11.

The calculation of texture features was also based on co-occurrence matrices using Haralick indices (Haralick 1979) for two different kernel sizes: 3 × 3 and 9 × 9, and using as input a brightness transformation of the original RGB image calculated as:

$$\mathrm{BRG} = [(299 \times \mathrm{R}) + (587 \times \mathrm{G}) + (114 \times \mathrm{B})]/1000.$$

Texture measures based on structural feature set (SFS; Xin et al. 2007) were also calculated using the same bright-

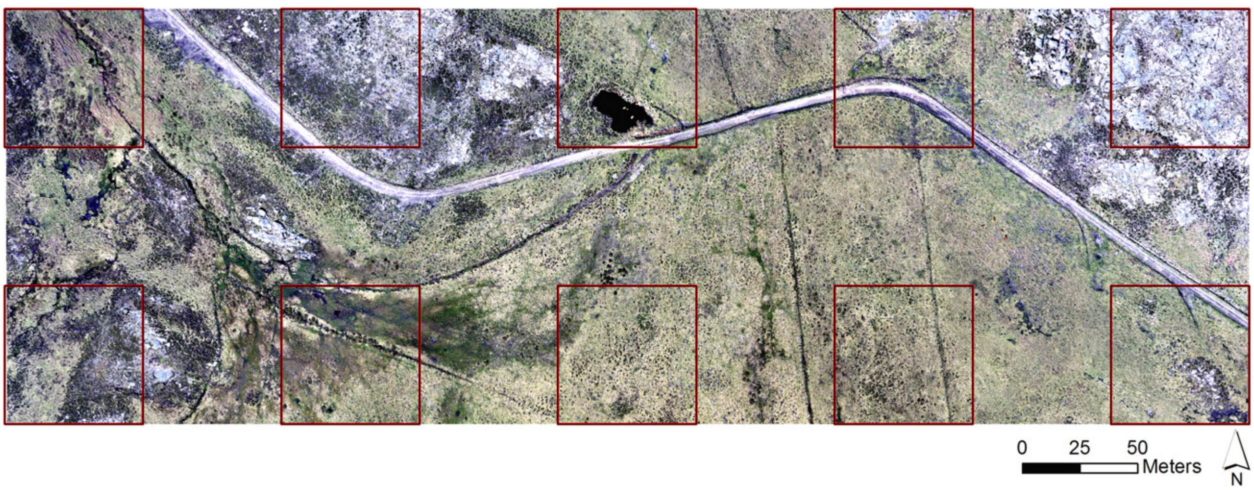

Fig. 4. Sample units (red quadrats) over the original colour image obtained with the UAV camera. The image evidences herbaceous (grassland) and woody (scrub) vegetation occurring in dense, complex mosaics, as well as extensive rock outcrops and some linear elements, such as water lines and tracks.

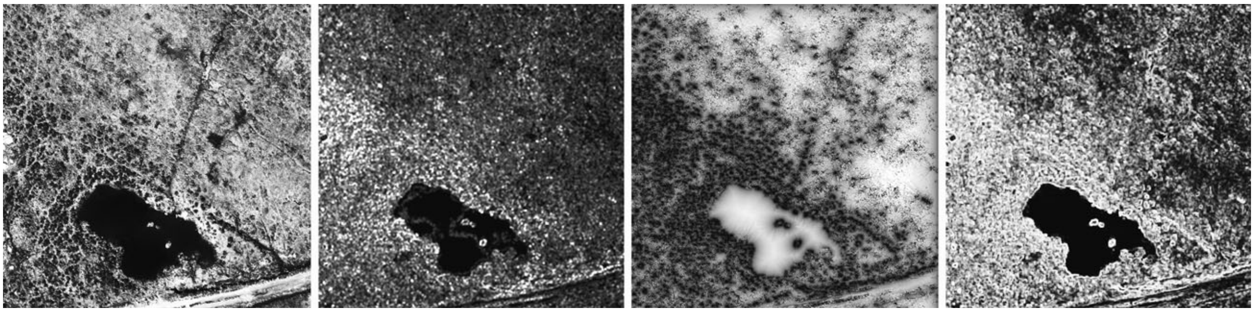

Fig. 5. Example of colour and texture features for a sample unit. From left to right: original red colour channel, Haralick, SFS and local statistics texture features evidencing small-scale differences and fine discrimination of herbaceous (grassland), woody (scrub) vegetation and a pond.

ness transformation. Both Haralick and SFS features were calculated using Orfeo Toolbox (CNES 2014).

Furthermore, a set of surface elevation features was obtained from the DSM by calculating the mean and standard-deviation features for three different kernel sizes: 5 × 5, 9 × 9 and 15 × 15, representing surface ruggedness. Surface curvature measures were also calculated to highlight surface convexity or concavity (Jenness 2013).

Random forest classifier training and validation

In this test, a pixel-based supervised classification framework was employed by combining ground truth training data with several colour, texture and surface features to produce an ensemble RF classifier (Breiman 2001). This algorithm was selected after a preliminary performance comparison between several other classification methods, namely: support vector machines, neural networks, k-nearest neighbour, generalized boosted model and C5.0. In this test, RF attained the highest accuracy and Kappa values (see detailed information in Appendix S4), and hence was selected to conduct the study. The R software package (R Foundation for Statistical Computing, Vienna, AT; http://www.r-project.org) was used for developing all image classification routines, in particular with the *randomForest* library (Liaw & Wiener 2002).

This stage started by generating 50 training and 50 validation data sets, each containing a stratified random draw of 10^5 pixels sampled from each digitized field-surveyed sample unit (SU). For each SU, 10^4 pixels were sampled proportional to stratum area allocation, using the previously defined classes as strata and ensuring that training pixels were not included in test sets. Due to the relatively large number of features and aiming to decrease multicollinearity and enhance processing speed, Spearman non-parametric correlation analysis was performed and features with very high correlation ($\rho \geq 0.9$) were initially discarded. Following this step, a preliminary RF classifier was devised and feature importance measures calculated. After some testing, only the 20 best features (Table 3) were kept, thus greatly reducing computation time and increasing classifier performance (not shown).

Using only the selected features, the final RF classifiers were developed for the previously generated training data sets. Using each trained RF classifier, we predicted the target classes for the entire area and ensembled the results through majority voting (i.e. for each pixel, the class most often predicted was maintained in the final map). Feature importance values were calculated and averaged across all training data sets using the total decrease in node impurities measured with the Gini index (Liaw & Wiener 2002).

To evaluate classification performance, we used the validation data sets and calculated several classification performance indices (Jolliffe & Stephenson 2003): overall accuracy, Heidke skill score, Peirce skill score, Gerrity skill score (see Appendix S5 for more details). To evaluate classification performances at class level, both producer and user accuracies were calculated.

We also compared producer and user accuracy values obtained with our UAV-based methodology to values collected from a semi-systematic literature review on the state-of-the-art of habitat classification and mapping in the context of Natura 2000 (25 articles were reviewed and two discarded for comparison purposes; see Fig. 6). To allow a meaningful comparison, this compilation focused only on habitat types similar to those analysed in this study, such as grasslands/meadows (62xx/64xx/65xx; 15 articles) and heathlands (40xx; eight articles). See also Appendix S6 for detailed information.

Results

Performance of the classification approach

Test results revealed a fairly good mean overall accuracy, equal to 0.89 (Table 1). Complementarily, other performance metrics also recorded overall good agreement between the predicted classes and validation data, with Gerrity skill score recording the highest value (0.86), followed by the Peirce skill score (0.86) and, finally,

Applied Vegetation Science
Doi: 10.1111/avsc.12204

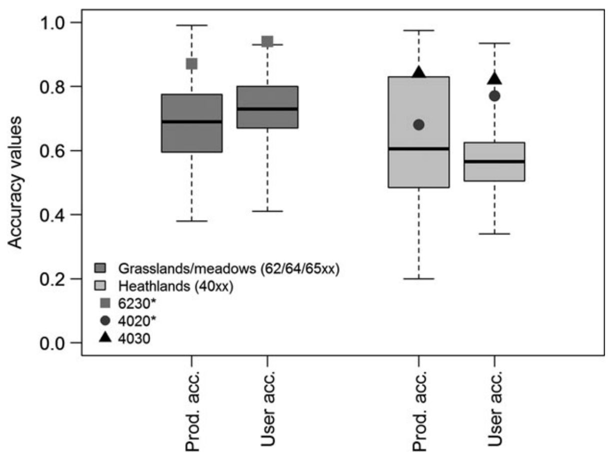

Fig. 6. Boxplot containing the distribution of producer and user accuracy values collected from research articles on the subject of habitat classification for similar habitat types, such as grasslands/meadows (62xx/64xx/65xx; *n* = 15 articles, grey colour) and heathlands (40xx; n = 8 articles, light grey). Boxes represent the 25%, 50% and 75% quartiles and whiskers the minimum and maximum values. Overlapped points display producer and user accuracy values obtained from the tested UAV-based classification for habitat types 6230* (squares), 4020* (circles) and 4030 (triangles).

Table 1. Overall validation measures averaged across all 50 data sets.

	Average	SD
ACC	0.89	0.0010
HSS	0.84	0.0014
PSS	0.86	0.0015
GSS	0.86	0.0018

ACC, overall accuracy; HSS, Heidke skill score; PSS, Peirce skill score; GSS, Gerrity skill score.

recording a lower performance, the Heidke skill score (0.84). In general, as shown by SD values, overall classification performance measures displayed low variability across validation sets.

High values of producer and user accuracy were obtained for habitat type 6230*, as well as for bare rock and for ponds (Table 2, Appendix S7). Other water surfaces/lines, such as temporary streams, drainage channels or small puddles, occurring mostly in the west side of the area, obtained good accuracy values. Habitat type 4020* and bare soil attained moderate producer accuracy values (respectively, 0.68 and 0.65) and slightly better accuracy at user level (0.77 and 0.80). Degraded versions of some habitat types, such as 6230*, were also discriminated with fairly good accuracy. Isolated patches of habitat type 4030, as well as patches of this habitat interspersed with bare rock, in poor conservation state, obtained good discrimination accuracy in the test. Results from the analysis of SD values showed low variability in producer and user accuracy across validation sets.

Feature importance ranking for habitat classification

Importance metrics calculated from the RF algorithm allowed ranking features according to their relative contribution to classification (Table 3). The ranking clearly highlighted the importance of surface elevation textures calculated with different kernel sizes. These features show the complex patterning of vegetation types occurring with varying densities at different elevations in the test area (Fig. 7a). Lower roughness/variability in surface values occurred (as expected) for the herbaceous habitat type 6230*, increasing up to tall shrub habitat type 4030 (Fig. 7c). Band ratio textures, especially B/R ratio, also recorded high importance, thus greatly contributing to discriminate classes. The B/R ratio texture displayed a fairly good separation between habitat type 4030 and habitat types 4020*/6230*, both exhibiting on average higher values for this variable (Fig. 7b). Ranking also showed that multiple band ratios based on several band combinations were useful for developing the RF classifier. Also ranking in the top five is the SFS WMean feature, showing that this type of texture descriptor was rather important for classification purposes. Average values for this texture descriptor showed moderate differentiation considering habitat types 4020* (with lowest WMean values), 4030 up to 6230 (recording the highest WMean values among these classes; Fig. 7d). Although with less relative contribution, local statistics calculated from raw colour channels using the mean and the variance as texture descriptors were included within the top ten of the ranking.

Table 2. Average producer and user accuracy values for each class.

	4020*	4030	6230*	6230* Degraded	Bare Rock	Bare Rock / 4030 Degraded	Bare Soil	Tracks	Water Surfaces / Water Lines	Ponds
Average Prod. acc.	0.68	0.84	0.96	0.87	0.94	0.80	0.65	0.90	0.77	0.97
Prod. Acc. SD	0.0079	0.0053	0.0013	0.0037	0.0023	0.0074	0.0072	0.0063	0.0198	0.0082
Average User Acc.	0.77	0.82	0.91	0.94	0.95	0.82	0.80	0.91	0.83	0.97
User Acc. SD	0.0070	0.0056	0.0015	0.0031	0.0026	0.0055	0.0060	0.0067	0.0133	0.0080

Values were aggregated using the mean ± SD across the 50 validation datasets.

Table 3. Average feature importance and overall ranking for calibrating the RF-based classifiers.

Rank	Mean Decrease Gini	Feature Acronym	Feature Description	Input and Texture Parameters
1	6573.2	DSM_SurfElevation_MN_R15	Surface elevation texture	DSM, mean, 15 × 15
2	6399.5	DSM_SurfElevation_MN_R9	Surface elevation texture	DSM, mean, 9 × 9
3	6328.4	DSM_SurfElevation_MN_R5	Surface elevation texture	DSM, mean, 5 × 5
4	4961.3	BR_Ratio_AVG_k11	Band ratio texture	B/R ratio, mean, 11 × 11
5	4695.5	SFS_WMean_LT100	SFS	Brightness transform, WMean, Spectral threshold = 100
6	4451.2	LS_Mean_CH1_RD9	Local statistics	R band, mean, 9 × 9
7	4014.1	LS_Var_CH3_RD9	Local statistics	B band, variance, 9 × 9
8	3896.3	LS_Mean_CH2_RD9	Local statistics	G band, mean, 9 × 9
9	3800.2	RB_Ratio_AVG_k11	Band ratio texture	R/B ratio, mean, 11 × 11
10	3486.8	LS_Mean_CH3_RD9	Local statistics	B band, mean, 9 × 9
11	3439.3	B_BGR_Ratio_AVG_k11	Band ratio texture	B/(B+R+G) ratio, mean, 11 × 11
12	3210.1	HC_HG_LGRE_XR9_YR9	Haralick texture	Brightness transform, Low Grey-Level Run Emphasis, 9 × 9
13	3047.1	HC_HG_SRLGE_XR9_YR9	Haralick texture	Brightness transform, Short Run Low Grey-Level Emphasis, 9 × 9
14	2895.9	DSM_SurfElevation_SD_R15	Surface elevation texture	DSM, SD, 15 × 15
15	2817.1	BG_Ratio_AVG_k11	Band ratio texture	B/G ratio, mean, 11 × 11
16	2495.9	R_RGB_Ratio_AVG_k11	Band ratio texture	R/(R+G+B) ratio, mean, 11 × 11
17	2246.9	R_BG_Ratio_AVG_k11	Band ratio texture	R/(B+G) ratio, mean, 11 × 11
18	2217.7	DSM_SurfElevation_SD_R9	Surface elevation texture	DSM, SD, 9 × 9
19	2213.4	GB_Ratio_AVG_k11	Band ratio texture	G/B ratio, mean, 11 × 11
20	1963.9	BR_Ratio_AVG_k5	Band ratio texture	B/R ratio, mean, 5 × 5

Results are aggregated across all training rounds.

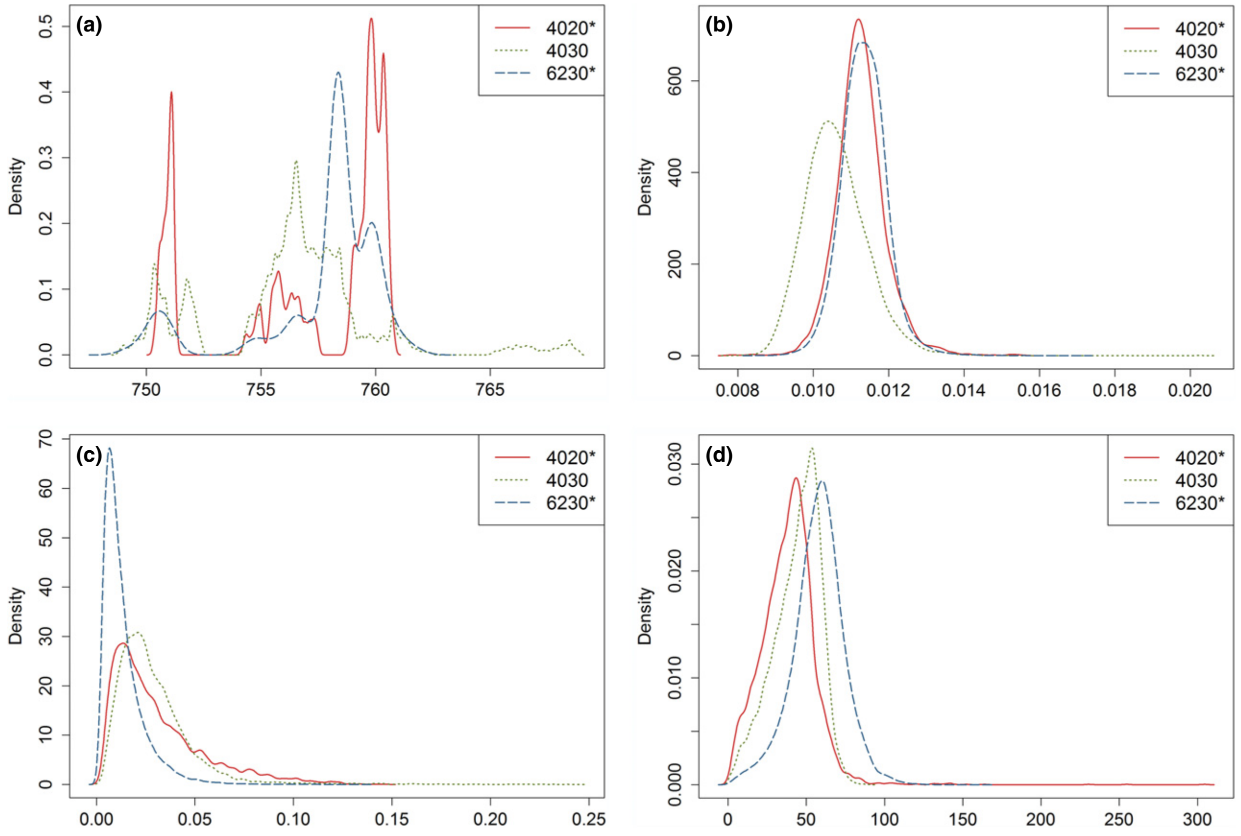

Fig. 7. Density plots for some of the most important features (Table 3) used to calibrate the RF classifiers, showing separation between the three habitat types in the study. (**a**) Surface elevation texture, Mean, 15 × 15; (**b**) R/B band ratio texture, Mean, 11 × 11; (**c**) Surface elevation texture, SD, 15 × 15; (**d**) SFS, Brightness band, WMean, Spectral threshold = 100.

Applied Vegetation Science
Doi: 10.1111/avsc.12204

Haralick texture metrics had the lowest scores, displaying a relatively lower contribution to discriminate classes. Overall in this test, larger kernel sizes used to calculate texture features such as 9 × 9, 11 × 11 up to 15 × 15 (when compared to 3 × 3 or 5 × 5 sizes), as well as the mean used as an aggregate function, were considered the most important.

Distribution and extent of habitat types in the study area

The distribution and spatial arrangement of the classes in the test area are illustrated in Fig. 7. From the classified image, it is possible to visualize that the western portion of the study area is far more complex, with reticulated vegetation patterning intercalated with bare soil and shallow water puddles in concave areas, or bare rock in upper areas with higher slopes. Habitat type 6230* is by far the predominant class, covering an estimated area of 5.88 ha, which comprises 60.63% of the test site (Table 4) and represents the matrix of the mosaic.

Table 4. Percentage cover and area (in ha) of each class in the study area.

Class	% Cover	Area (ha)
4020*	5.41	0.53
4030	8.50	0.82
6230*	60.63	5.88
6230* Degraded/Bare Soil	4.26	0.41
Bare Rock	7.01	0.68
Bare Rock/4030 Degraded	5.16	0.50
Bare Soil	4.87	0.47
Tracks	1.94	0.19
Water Surfaces/Water Lines	1.96	0.19
Ponds	0.25	0.02

A degraded version of this habitat type, with a less favourable habitat condition (0.41 ha, or 4.26% of the study area), occurs mostly in a single large patch located in the southwest portion of the site. Habitat type 4020* and all other classes occur scattered within this matrix, occupying <10% of the area individually. Small mosaics of drier areas, dominated by bare rock, bare soil and dry heath, are easily distinguished from wet areas with the focal priority habitat types and small water surfaces (Figs 2 and 8). Overall, these results are consistent with the high grazing pressure observed in the field and possibly related to the concentration of pastoral activities in these highly productive mosaics.

Discussion

Strengths and caveats of the methodology

Developing methods for fine-scale mapping of valuable habitats based on UAV imagery represents a step forward in ecological assessment (Anderson & Gaston 2013). These images allow the capture of a high level of detail and portray the 2D and 3D structure of vegetation from digital surface elevation models. In this test, we developed a UAV-based assessment methodology to map the extent of Natura 2000 priority habitats, obtaining good overall accuracy, in spite of some decrease in classification performance in situations of high interspersion of vegetation types. However, comparisons with officially reported national statistics of habitat extent and distribution could not be performed due to

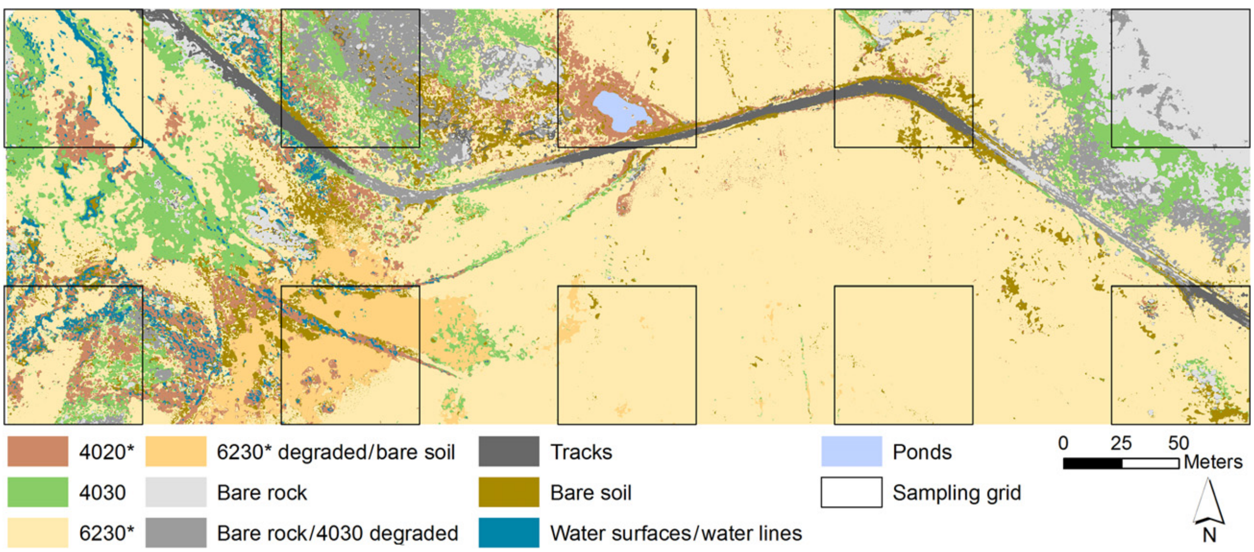

Fig. 8. Map representation of the study area, displaying the cover of different classes as predicted by ensembling of RF classifiers.

Doi: 10.1111/avsc.12204

the lack of updated information and the coarseness of existing databases.

At the class level, grasslands (habitat type 6230*), which are the vegetation matrix in the test-site, attained better results, while wet heath (4020*) obtained only moderate accuracy values as evaluated with test data. Misclassification of habitat type 4020* may be due to some degree of generalization in the definition of complex training areas, the patchiness of vegetation patterns in the study area, and the tendency of this habitat type to occur in intricate mosaics, with different species becoming locally dominant, thus hampering its correct identification and delineation both in the field and for classification purposes. Moreover, there were some difficulties in distinguishing dominant species of each type of vegetation with similar life forms. One such example is *Ulex europaeus* (subsp. *latebracteatus*) and *U. minor*, the first being dominant in habitat type 4030 (European dry heathlands) and the second dominating much of the patches of habitat type 4020* (temperate wet heath). Another problematic example is distinguishing among species of perennial grass, such as *A. capillaris*, *A. hesperica* or *N. stricta*. *A. capillaris* can be found in a large diversity of habitats and is dominant in degraded versions of habitat type 6230* (*Nardus* grasslands) and in other types of grassland not corresponding to any particular Annex I habitat type.

In further fine-tuning of the methodology, most of these problems could potentially be resolved using contextual information, e.g. percentage of rocks in neighbouring areas may be a helpful indicator to determine the species of *Ulex*, and consequently the particular Annex I habitat type. Regarding discrimination of perennial grasses, the co-existence with other ubiquitous mesophytic species, such as *Pteridium aquilinum*, may also be a valuable indicator.

When compared to reference producer and user accuracy values collected from the literature (Fig. 6), our UAV-based approach presents above-median performance for both grassland and heathland habitats (in most cases >75% quartile, with the exception of producer accuracy for habitat type 4020*). Nevertheless, these comparisons must be interpreted only as an indirect baseline, since no directly comparable results (i.e. applications using UAV imagery for similar or the same habitat types) were found in the literature, and also due to differences in input remote sensing data (e.g. RapidEye, QuickBird, Landsat, LiDAR) classification approach (pixel vs object-based) and classification algorithms (e.g. support vector machines, maximum likelihood, nearest neighbour; see Appendix S6 for more details). Comparison results suggest that UAV low-spectral resolution may be partially compensated by its very high, sub-decimetre spatial resolution. They also highlight the cost-effectiveness of UAV-based methodologies, since most habitat classification approaches currently employ very high-resolution satellite imagery (e.g. Förster et al. 2008; Hernando et al. 2012; Buck et al. 2015) with comparatively higher acquisition costs.

This methodology also allowed us to distinguish several meaningful classes as well as some degraded patches of particular habitat types in a quite challenging, dynamic and dense vegetation mosaic. In some cases, we were able to detect the presence of dry heathland, bare soil patches or shallow water puddles neighbouring habitat type 4020*, possibly identifying situations where the habitat occurs in less favourable conservation conditions, likely due to over-grazing and localized used of fire. We were also able to identify patches of habitat type 6230* exhibiting a less favourable habitat condition, related to visible changes in the typical vegetation structure and species assembly (as verified during in-field surveys) and identifiable in UAV imagery as higher textural heterogeneity or chromatic alterations due to higher shrub density (or encroachment) and presence of open soil (see Figs 2 and 4). This type of information may prove useful for management and conservation of the focal habitats, and is still poorly explored in ecological applications (with exceptions, e.g. Spanhove et al. 2012) of UAV imagery.

Test results also highlighted the adequacy of the RF algorithm to produce a classifier capable of coping both with the large amount and high dimensionality of imagery data (see also Appendix S4). In addition, low variability of validation metrics across test data sets further showed the high generalization ability of this algorithm. Using sampling strategies to generate training/test data, such as those developed in our methodology, and performing an initial selection of best features, allowed us to improve classification accuracy and reduce computation time.

Our results strongly emphasize the usefulness of features derived from photogrammetric DSMs, as well as different texture features calculated from colour imagery, as observed in previous UAV applications (e.g. Laliberte & Rango 2008, 2009). These features allowed the inclusion of useful vicinal and context information in the classification for identifying different vegetation/habitat types and their edges. Computationally inexpensive texture features such as those based on the calculation of local statistics (e.g. mean, variance) for various kernel sizes obtained better results in comparison, e.g. with Haralick features, which require much longer computation time and resources. Band ratios, previously highlighted as important in the context of UAV habitat/species classification (e.g. Dunford et al. 2009; Laliberte & Rango 2011), also obtained better results when compared to raw input data. This may be due to the ability of band ratios to remove much of the effect of illumination and enhance (or reveal) latent information

Applied Vegetation Science
Doi: 10.1111/avsc.12204

when there is an inverse relationship between two spectral responses to the same biophysical phenomenon (Campbell & Wynne 2011).

Moreover, the use of near-infrared images (not available in our UAV platform) could be used to allow calculation of vegetation indices (Anderson & Gaston 2013; Knoth et al. 2013; Calviño-Cancela et al. 2014) and improve assessment of habitat extent and condition. These data, combined with a 3D representation of vegetation obtained through a canopy height model (Dandois & Ellis 2013), could potentially contribute to further enhance classification accuracy and the ability to diagnose the condition of some habitat types in fine-scale mosaics.

Applications in monitoring small-scale habitat mosaics and future directions

The results obtained in this test, employing UAV-based colour imagery and a DSM for the classification of a complex and dynamic habitat mosaics, revealed that the methodology can successfully discriminate a relatively large number of classes with high to very high levels of accuracy. This suggests that it can provide robust estimates of class/habitat diversity, as well as of the extent of each habitat type, which in turn may be particularly useful for supporting mandatory Natura 2000 reporting obligations (Vanden Borre et al. 2011), especially in EU member states currently lacking detailed assessments and/or standardized procedures for such a task. UAV-based assessments show high potential to complement previous research in the detection and mapping of Natura 2000 habitats currently employing satellite imagery from moderate (Díaz Varela et al. 2008) to very high (Förster et al. 2008; Hernando et al. 2012; Schmidt et al. 2014; Buck et al. 2015) spatial resolution, hyperspectral sensors (Haest et al. 2010; Chan et al. 2012; Spanhove et al. 2012), radar satellite data (Schuster et al. 2011, 2015) and LiDAR (Bässler et al. 2011; Zlinszky et al. 2014). We argue that well planned, standardized and systematic UAV surveying over a statistically sound selection of sites could help to develop a monitoring system that could inform the extent, connectivity, habitat condition and trends of Natura 2000 habitats in a reproducible fashion and allow a reduction in running costs and operational complexity of image acquisition (Anderson & Gaston 2013; Mancini et al. 2013; Calviño-Cancela et al. 2014). This would require the definition of highly standardized field methods incorporating botanical, vegetation and remote sensing expertise as a crucial step to bridge gaps between field and UAV-based remote sensing methods.

Covering much wider areas (by a factor of ten or 100) than that used in this pilot test (with roughly 10 ha) would be easily accomplished by adapting flight parameters, performing multiple flights and/or employing UAV platforms with higher operating ranges and autonomy (Anderson & Gaston 2013). Due to the diversity and adaptability of existing UAV platforms, it would be possible to extend surveying to other different small-scale habitat mosaics, such as dunes (Mancini et al. 2013), wetlands (Ishihama et al. 2012) or riparian ecosystems (Dunford et al. 2009). In order to adequately accomplish this, nature protection agencies and/or partner stakeholders should acquire suitable UAV equipment, train their staff in using this type of technology and develop semi-automated procedures for image post-processing and classification, thus making it easier and faster to analyse UAV data. In turn, long-term advantages of UAV-based ecological monitoring related to flexible flight scheduling, prompt availability of very high-resolution images, reduced acquisition costs, low or absent cloud contamination (Getzin et al. 2012; Anderson & Gaston 2013) and other factors could provide a cost-effective solution for conservation agencies.

Acknowledgements

This study was developed as part of the LIFE+ project 'Higro' (Demonstrative Actions for the Conservation of Priority Habitats in Northern Mountain Areas in Portugal; LIFE09NAT/PT/000043). João Gonçalves was supported by the Portuguese Foundation for Science and Technology (FCT; PhD grant nr. SFRH/BD/90112/2012). Rita Sousa-Silva is supported by a PhD grant from KU Leuven in the framework of the FORBIO Climate project, financed by BRAIN.be, Belgian Research Action through INterdisciplinary research. António T. Monteiro is supported through the Project 'Biodiversity, Ecology and Global Change', co-financed by North Portugal Regional Operational Programme 2007/2013 (ON.2 – O Novo Norte), under the National Strategic Reference Framework (NSRF), through the European Regional Development Fund (ERDF). A. Lomba is supported by the PFST through Post-Doctoral Fellowship SFRH/BPD/80747/2011. Bruno Marcos received support from FEDER/COMPETE and FCT through project grant 'IND_CHANGE' (PTDC/AAG-MAA/4539/2012 – FCOMP-01-0124-FEDER-027863).

References

Agisoft 2012. *Agisoft photoscan user manual, professional edition, v 0.9.0.* aiHit - Agisoft, Cork, IE.

Anderson, K. & Gaston, K.J. 2013. Lightweight unmanned aerial vehicles will revolutionize spatial ecology. *Frontiers in Ecology and the Environment* 11: 138–146.

Bässler, C., Stadler, J., Müller, J., Förster, B., Göttlein, A. & Brandl, R. 2011. LiDAR as a rapid tool to predict forest habitat types in Natura 2000 networks. *Biodiversity and Conservation* 20: 465–481.

Bielsa, I., Pons, X. & Bunce, B. 2005. Agricultural abandonment in the North Eastern Iberian Peninsula: the use of basic landscape metrics to support planning. *Journal of Environmental Planning and Management* 48: 85–102.

Bolliger, J., Kienast, F., Soliva, R. & Rutherford, G. 2007. Spatial sensitivity of species habitat patterns to scenarios of land use change (Switzerland). *Landscape Ecology* 22: 773–789.

Breiman, L. 2001. Random forests. *Machine Learning* 45: 5–32.

Brown, J., Kothari, A., Brown, J. & Kothari, A. 2011. Traditional agricultural landscapes and community conserved areas: an overview. *Management of Environmental Quality: An International Journal* 22: 139–153.

Buck, O., Millán, V.E.G., Klink, A. & Pakzad, K. 2015. Using information layers for mapping grassland habitat distribution at local to regional scales. *International Journal of Applied Earth Observation and Geoinformation* 37: 83–89.

Burkinshaw, A. & Bork, E. 2009. Shrub encroachment impacts the potential for multiple use conflicts on public land. *Environmental Management* 44: 493–504.

Calviño-Cancela, M., Méndez-Rial, R., Reguera-Salgado, J. & Martín-Herrero, J. 2014. Alien plant monitoring with ultralight airborne imaging spectroscopy. *PLoS One* 9: e102381.

Campbell, J.B. & Wynne, R.H. 2011. *Introduction to remote sensing*, 5th edn. Guilford Press, New York, NY, US.

Chan, J.C.-W., Beckers, P., Spanhove, T. & Borre, J.V. 2012. An evaluation of ensemble classifiers for mapping Natura 2000 heathland in Belgium using spaceborne angular hyperspectral (CHRIS/Proba) imagery. *International Journal of Applied Earth Observation and Geoinformation* 18: 13–22.

CNES 2014. *The ORFEO tool box software guide – updated for OTB-4.0*. Centre National d'Études Spatiales: Paris, FR.

Corbane, C., Lang, S., Pipkins, K., Alleaume, S., Deshayes, M., García Millán, V.E., Strasser, T., Vanden Borre, J., Toon, S. & Michael, F. 2015. Remote sensing for mapping natural habitats and their conservation status – new opportunities and challenges. *International Journal of Applied Earth Observation and Geoinformation* 37: 7–16.

Dandois, J.P. & Ellis, E.C. 2013. High spatial resolution three-dimensional mapping of vegetation spectral dynamics using computer vision. *Remote Sensing of Environment* 136: 259–276.

Díaz Varela, R.A., Ramil Rego, P., Calvo Iglesias, S. & Muñoz Sobrino, C. 2008. Automatic habitat classification methods based on satellite images: a practical assessment in the NW Iberia coastal mountains. *Environmental Monitoring and Assessment* 144: 229–250.

Dunford, R., Michel, K., Gagnage, M., Piégay, H. & Trémelo, M.L. 2009. Potential and constraints of unmanned aerial vehicle technology for the characterization of Mediterranean riparian forest. *International Journal of Remote Sensing* 30: 4915–4935.

European Commission 1992. *Council Directive 92/43/EEC of 21 May 1992 on the conservation of natural habitats and of wild fauna and flora, 1992L0043*. The Council of the European Communities, Brussels, BE.

Förster, M., Frick, A., Walentowski, H. & Kleinschmit, B. 2008. Approaches to utilising QuickBird data for the monitoring of NATURA 2000 habitats. *Community Ecology* 9: 155–168.

Franco, J.A. 1984. *Nova Flora de Portugal (Continente e Açores). Vol. II, Clethraceae-Compositae*. Author's Edition, Lisbon, PT.

Franco, J.A. & Afonso, M.R. 1998. *Nova Flora de Portugal (Continente e Açores). Vol. III (Fasc. II), Gramineae*. Escolar Editora, Lisbon, PT.

Getzin, S., Wiegand, K. & Schöning, I. 2012. Assessing biodiversity in forests using very high-resolution images and unmanned aerial vehicles. *Methods in Ecology and Evolution* 3: 397–404.

González-Orozco, C.E., Mulligan, M., Trichon, V. & Jarvis, A. 2010. Taxonomic identification of Amazonian tree crowns from aerial photography. *Applied Vegetation Science* 13: 510–519.

Goodall, D.W. & Perry, R.A. 2009. *Arid land ecosystems: volume 2, structure, functioning and management*. Cambridge University Press, Cambridge, UK.

Gross, J.E., Goetz, S.J. & Cihlar, J. 2009. Application of remote sensing to parks and protected area monitoring: introduction to the special issue. *Remote Sensing of Environment* 113: 1343–1345.

Gruijter, J.D., Brus, D., Bierkens, M. & Knotters, M. 2006. *Sampling for natural resource monitoring*. Springer, Berlin, DE.

Haest, B., Thoonen, G., Borre, J.V., Spanhove, T., Delalieux, S., Bertels, L., Kooistra, L., Mücher, C.A. & Scheunders, P. 2010. An object-based approach to quantity and quality assessment of heathland habitats in the framework of Natura 2000 using hyperspectral airborne images. In: Addink, E.A. & Coillie, F.M.B.V. (eds.) *GEOBIA 2010: geographic object-based image analysis*, pp. 6. GEOBIA/ISPRS, Ghent, BE.

Halada, L., Evans, D., Romão, C. & Petersen, J.-E. 2011. Which habitats of European importance depend on agricultural practices? *Biodiversity and Conservation* 20: 2365–2378.

Haralick, R.M. 1979. Statistical and structural approaches to texture. *Proceedings of the IEEE* 67: 786–804.

Hernando, A., Arroyo, L.A., Velázquez, J. & Tejera, R. 2012. Object-based image analysis for mapping Natura 2000 habitats to improve forest management. *Photogrammetric Engineering & Remote Sensing* 78: 991–999.

Huang, X., Zhang, L. & Li, P. 2007. Classification and extraction of spatial features in urban areas using high-resolution multispectral imagery. *IEEE Geoscience and Remote Sensing Letters* 4: 260–264.

Husson, E., Hagner, O. & Ecke, F. 2014. Unmanned aircraft systems help to map aquatic vegetation. *Applied Vegetation Science* 17: 567–577.

Immitzer, M., Atzberger, C. & Koukal, T. 2012. Tree species classification with Random forest using very high spatial resolution 8-band worldView-2 satellite data. *Remote Sensing* 4: 2661–2693.

Ishihama, F., Watabe, Y. & Oguma, H. 2012. Validation of a high-resolution, remotely operated aerial remote-sensing system for the identification of herbaceous plant species. *Applied Vegetation Science* 15: 383–389.

Jenness, J. 2013. *DEM surface tools for ArcGIS (surface_area.exe)*. Jenness Enterprises, Flagstaff, AZ.

Jolliffe, I.T. & Stephenson, D.B. 2003. *Forecast verification – a practitioner's guide in atmospheric science*, 1st edn. John Wiley & Sons, Chichester, UK.

Knoth, C., Klein, B., Prinz, T. & Kleinebecker, T. 2013. Unmanned aerial vehicles as innovative remote sensing platforms for high-resolution infrared imagery to support restoration monitoring in cut-over bogs. *Applied Vegetation Science* 16: 509–517.

Köhl, M., Magnussen, S. & Marchetti, M. 2006. *Sampling methods, remote sensing and GIS multiresource forest inventory*. Springer, Berlin, DE.

Laliberte, A. & Rango, A. 2008. Incorporation of texture, intensity, hue, and saturation for rangeland monitoring with unmanned aircraft imagery. In: Hay, G.J., Blaschke, T. & Marceau, D. (eds.) *GEOBIA proceedings*, pp. 4/C1. GEOBIA/ISPRS, Calgary, CA.

Laliberte, A.S. & Rango, A. 2009. Texture and scale in object-based analysis of subdecimeter resolution unmanned aerial vehicle (UAV) imagery. *IEEE Transactions on Geoscience and Remote Sensing* 47: 761–770.

Laliberte, A.S. & Rango, A. 2011. Image processing and classification procedures for analysis of sub-decimeter imagery acquired with an unmanned aircraft over arid rangelands. *GIScience & Remote Sensing* 48: 4–23.

Liaw, A. & Wiener, M. 2002. Classification and regression by randomForest. *R News* 2: 18–22.

MacDonald, D., Crabtree, J.R., Wiesinger, G., Dax, T., Stamou, N., Fleury, P., Gutierrez Lazpita, J. & Gibon, A. 2000. Agricultural abandonment in mountain areas of Europe: environmental consequences and policy response. *Journal of Environmental Management* 59: 47–69.

Mancini, F., Dubbini, M., Gattelli, M., Stecchi, F., Fabbri, S. & Gabbianelli, G. 2013. Using unmanned aerial vehicles (UAV) for high-resolution reconstruction of topography: the structure from motion approach on coastal environments. *Remote Sensing* 5: 6880–6898.

Nagendra, H., Lucas, R., Honrado, J.P., Jongman, R.H.G., Tarantino, C., Adamo, M. & Mairota, P. 2013. Remote sensing for conservation monitoring: assessing protected areas, habitat extent, habitat condition, species diversity, and threats. *Ecological Indicators* 33: 45–59.

Ninyerola, M., Pons, X. & Roure, J.M. 2005. *Atlas Climático Digital de la Península Ibérica. Metodología y aplicaciones en bioclimatología y geobotánica*. Universidad Autónoma de Barcelona, Bellaterra, ES.

Pal, M. 2005. Random forest classifier for remote sensing classification. *International Journal of Remote Sensing* 26: 217–222.

Peel, M.C., Finlayson, B.L. & McMahon, T.A. 2007. Updated world map of the Köppen–Geiger climate classification. *Hydrology and Earth Systems Science* 11: 1633–1644.

Permuter, H., Francos, J. & Jermyn, I. 2006. A study of Gaussian mixture models of color and texture features for image classification and segmentation. *Pattern Recognition* 39: 695–706.

Plieninger, T. 2006. Habitat loss, Fragmentation, and Alteration – quantifying the impact of land-use changes on a Spanish Dehesa landscape by use of aerial photography and GIS. *Landscape Ecology* 21: 91–105.

Rodriguez-Galiano, V.F. & Chica-Rivas, M. 2012. Evaluation of different machine learning methods for land cover mapping of a Mediterranean area using multi-seasonal Landsat images and Digital Terrain Models. *International Journal of Digital Earth* 7: 492–509.

Rodriguez-Galiano, V.F., Ghimire, B., Rogan, J., Chica-Olmo, M. & Rigol-Sanchez, J.P. 2012. An assessment of the effectiveness of a random forest classifier for land-cover classification. *ISPRS Journal of Photogrammetry and Remote Sensing* 67: 93–104.

Romero García, A.T., Blanca López, G. & Morales Torres, C. 1988. Revisión del género Agrostis L. (Poaceae) en la península ibérica. *Ruizia* 7: 1–160.

Sala, O.E., Stuart Chapin, F. III, Armesto, J.J., Berlow, E., Bloomfield, J., Dirzo, R., Huber-Sanwald, E., Huenneke, L.F., Jackson, R.B., (. . .) & Wall, D.H. 2000. Global biodiversity scenarios for the year 2100. *Science* 287: 1770–1774.

Schmidt, T., Schuster, C., Kleinschmit, B. & Forster, M. 2014. Evaluating an intra-annual time series for grassland classification – how many acquisitions and what seasonal origin are optimal? *IEEE Journal of Selected Topics in Applied Earth Observations and Remote Sensing* 7: 3428–3439.

Schuster, C., Ali, I., Lohmann, P., Frick, A., Förster, M. & Kleinschmit, B. 2011. Towards detecting swath events in TerraSAR-X time series to establish NATURA 2000 grassland habitat swath management as monitoring parameter. *Remote Sensing* 3: 1308–1322.

Schuster, C., Schmidt, T., Conrad, C., Kleinschmit, B. & Förster, M. 2015. Grassland habitat mapping by intra-annual time series analysis – comparison of RapidEye and TerraSAR-X satellite data. *International Journal of Applied Earth Observation and Geoinformation* 34: 25–34.

Spanhove, T., Vanden Borre, J., Delalieux, S., Haest, B. & Paelinckx, D. 2012. Can remote sensing estimate fine-scale quality indicators of natural habitats? *Ecological Indicators* 18: 403–412.

Vanden Borre, J., Paelinckx, D., Mücher, C.A., Kooistra, L., Haest, B., De Blust, G. & Schmidt, A.M. 2011. Integrating remote sensing in Natura 2000 habitat monitoring: prospects on the way forward. *Journal for Nature Conservation* 19: 116–125.

Waldhardt, R., Simmering, D. & Otte, A. 2004. Estimation and prediction of plant species richness in a mosaic landscape. *Landscape Ecology* 19: 211–226.

Weiers, S., Bock, M., Wissen, M. & Rossner, G. 2004. Mapping and indicator approaches for the assessment of habitats at different scales using remote sensing and GIS methods. *Landscape and Urban Planning* 67: 43–65.

Xin, H., Liangpei, Z. & Pingxiang, L. 2007. Classification and extraction of spatial features in urban areas using high-resolution multispectral imagery. *IEEE Geoscience and Remote Sensing Letters* 4: 260–264.

Zhang, C. & Xie, Z. 2013. Object-based vegetation mapping in the Kissimmee River watershed using HyMap data and machine learning techniques. *Wetlands* 33: 233–244.

Zlinszky, A., Schroiff, A., Kania, A., Deák, B., Mücke, W., Vári, Á., Székely, B. & Pfeifer, N. 2014. Categorizing grassland vegetation with full-waveform airborne laser scanning: a feasibility study for detecting Natura 2000 habitat types. *Remote Sensing* 6: 8056–8087.

Supporting Information

Additional Supporting Information may be found in the online version of this article:

Appendix S1. Test-site photographs recorded during in-field campaigns.

Appendix S2. Spectral sensitivity data for Canon cameras.

Appendix S3. Features used for supervised image classification.

Appendix S4. Preliminary cross-validation results comparing the performance of candidate classification algorithms.

Appendix S5. Overall classification performance measures.

Appendix S6. References used for comparing producer and user accuracy values.

Appendix S7. Confusion matrix calculated from test set 1.

Applied Vegetation Science
Doi: 10.1111/avsc.12204